SUPPLEMENTAL INFROMATION

p300-Mediated Lysine 2-Hydroxyisobutyrylation Regulates Glycolysis

He Huang,[1,5] Shuang Tang,[2,5] Ming Ji,[2,5] Zhanyun Tang,[3] Miho Shimada,[3] Xiaojing Liu,[4] Shankang Qi,[1] Jason W. Locasale,[4] Robert G. Roeder,[3] Yingming Zhao,[1,*] and Xiaoling Li [2,6,*]

[1]Ben May Department for Cancer Research, The University of Chicago, Chicago, IL 60637

[2]Signal Transduction Laboratory, National Institute of Environmental Health Sciences, Research Triangle Park, NC 27709

[3]Laboratory of Biochemistry and Molecular Biology, The Rockefeller University, New York, NY 10065

[4]Department of Pharmacology and Cancer Biology, Duke Cancer Institute, Duke Molecular Physiology Institute, Duke University School of Medicine, Durham, NC 27710

[5]These authors contribute equally to this work.

[6]Lead contact

* Correspondence: X.L., lix3@niehs.nih.gov, Y. Z., yingming.zhao@uchicago.edu

Running title: p300 regulates glycolysis through lysine 2-hydroxyisobutyrylation

Key words: p300, lysine 2-hydroxyisobutyrylation, glycolysis, cell survival

SUPPLEMENTAL FIGURE LEGENDS

Figure S1. p300 Catalyzes Histone Khib, Related to Figure 1.

(A) Dose-dependent inhibition of p300 by C646 reduces Khib and Kac levels of histones in cells. Hela cells and HEK293T cells were treated with a p300 inhibitor C646 at indicated concentration for 24 hours, and the Khib and Kac levels of histones were analyzed by immuno-blotting with indicated antibodies.

(B) Schematic of the p53 dependent cell-free transcription assay.

Figure S2. Systematic Profiling of Kac and Khib proteomes in WT and P300 KO Cells, Related to Figure 2.

(A) Schematic representation of experimental workflow for the SILAC quantification of p300-regulated acetylome and 2-hydroxyisobutyrylome.

(B) Venn diagram showing the overlap between replications.

(C) Histogram showing the Kac and Khib site distribution.

(D) p300 catalyzes acetylation and 2-hydroxyisobutyrylation on distinct lysine residues in a variety of protein substrates. Venn diagram showing overlap of the identified total Kac and Khib sites in HCT116 cells.

(E) The Venn diagrams show cellular compartment distribution of all identified Khib and Kac proteins.

Figure S3. p300 deficiency results in defective glycolysis, Related to Figure 4.

(A) p300 KO HCT116 cells have alteration in glycolysis or gluconeogenesis. WT and p300 KO HCT116 cells were cultured in complete medium or glucose free medium for 6 hours. The relative abundance of metabolites involved in glycolysis, TCA cycle, PPP, and glutamine pathway was displayed by the heat map.

(B) Deletion of p300 significantly alters glycolysis or gluconeogenesis. The metabolites with fold change (KO/WT<0.5) and p<0.05 (n=3) were analyzed by the pathway enrichment analysis and the pathway topology analysis in the Pathway Analysis module of MetaboAnalyst 3.0.

(C) p300 KO HCT116 cells have altered glycolysis and TCA cycle when cultured in complete medium.

(D) Deletion of p300 in HCT116 cells using Crispr/Cas technology reduces glycolysis. The glycolysis activity was analyzed by the Seahorse analyzer (n=4, values are expressed as mean ±SEM). p300 Crispr KO HCT116 cells were generated as described in the STAR Methods.

Figure S4. p300-mediated 2-hydroxyisobutyrylation regulates glycolysis in HCT116 cells, Related to Figure 5.

(A) p300 KO HCT116 cells have normal expression levels of most genes involved in glucose metabolism. Relative mRNA levels of genes involved in glycolysis in WT and p300 KO HCT116 cells (n=3 from 2 pairs of WT and p300 HCT116 cells, *p<0.05, values are expressed as mean ±SEM).

(B) The protein levels of ENO1, PFKM, and GLUT1 in WT and p300 KO HCT116 cells.

(C) The Khib level of endogenous PFKM is reduced in p300 deficient HCT116 cells. Endogenous PFKM proteins were immuno-purified WT, p300 KO, p300 crispr KO HCT116 cells, and the Khib and Kac levels of the purified proteins were analyzed.

(D) The p300-targeted Khib sites are on the surface of ENO1 (PDB entry 2PSN). The structure of ENO1 dimer is shown as cartoon and the modified lysine residues are marked as purple.

(E) The K281R mutant ENO1 protein has reduced Khib levels. WT HA-ENO1 or K281R HA-ENO1 proteins were immune-purified using a mouse monoclonal anti-HA antibody (sc-7392) from HCT116 and HEK293T cells, and the Khib, Kac, and total HA-ENO1 levels of the purified proteins were analyzed using indicated rabbit antibodies.

(F) The K281R mutant ENO1 protein displays a comparable stability as WT ENO1 in cells. HCT116 cells expressing WT HA-ENO1 or K281R HA-ENO1 protein were treated with 100 μg/ml cycloheximide (CHX) for indicated times and the levels of these protein were analyzed by immuno-blotting using anti-HA antibodies.

Figure S5. p300 deficiency in HEK293T cells and SW620 cells reduces glycolysis and results in hyper-sensitivity glucose depletion, Related to Figure 7.

(A) Protein levels of HA-ENO1 in WT and p300 KO HEK293T cells transfected with either empty vector (Vec) or constructs expressing WT HA-ENO1 or K281R HA-ENO1 proteins.

(B) mRNA levels of ENO1 in HEK293T cells transfected with a construct expressing control shRNA (shControl), constructs expressing shRNA against 3' UTR of ENO1 (shENO1), the shENO1 constructs together with a construct containing the coding region of the WT ENO1 gene (shENO1 WT ENO1), or the shENO1 constructs together with a construct containing the coding region of the K281R ENO1 gene (shENO1 K281R ENO1). The mRNA levels of ENO1 in these three cells were analyzed by qPCR. Please note that constructs expressing shRNA against 3' UTR of ENO1 efficiently knocked down the endogenous ENO1 mRNA (probed by primers targeting ENO1 3'UTR), and constructs containing the coding region of WT or K281R ENO1 genes brought the total ENO1 levels back to the control levels (probed by primers targeting the ENO1 coding region).

(C) WT and K281T ENO1 have comparable protein levels in shENO1 HEK293T cells.

(D) shRNA-medicated knockdown of p300 in SW620 cells. The protein levels of p300 in WT and p300 knockdown cells were analyzed by immuno-blotting.

(E) p300 knockdown SW620 cells have reduced ENO1 activity (n=3, values are expressed as mean ±SEM).

(F-G) p300 knockdown SW620 cells are hypersensitive to glucose depletion. WT and p300 knockdown cells were cultured for 72 hours in indicated medium, and cell death was analyzed by

FACS as described in STAR Methods (n=3, *p<0.05, values are expressed as mean ±SEM). Bar in (F), 100 μm.

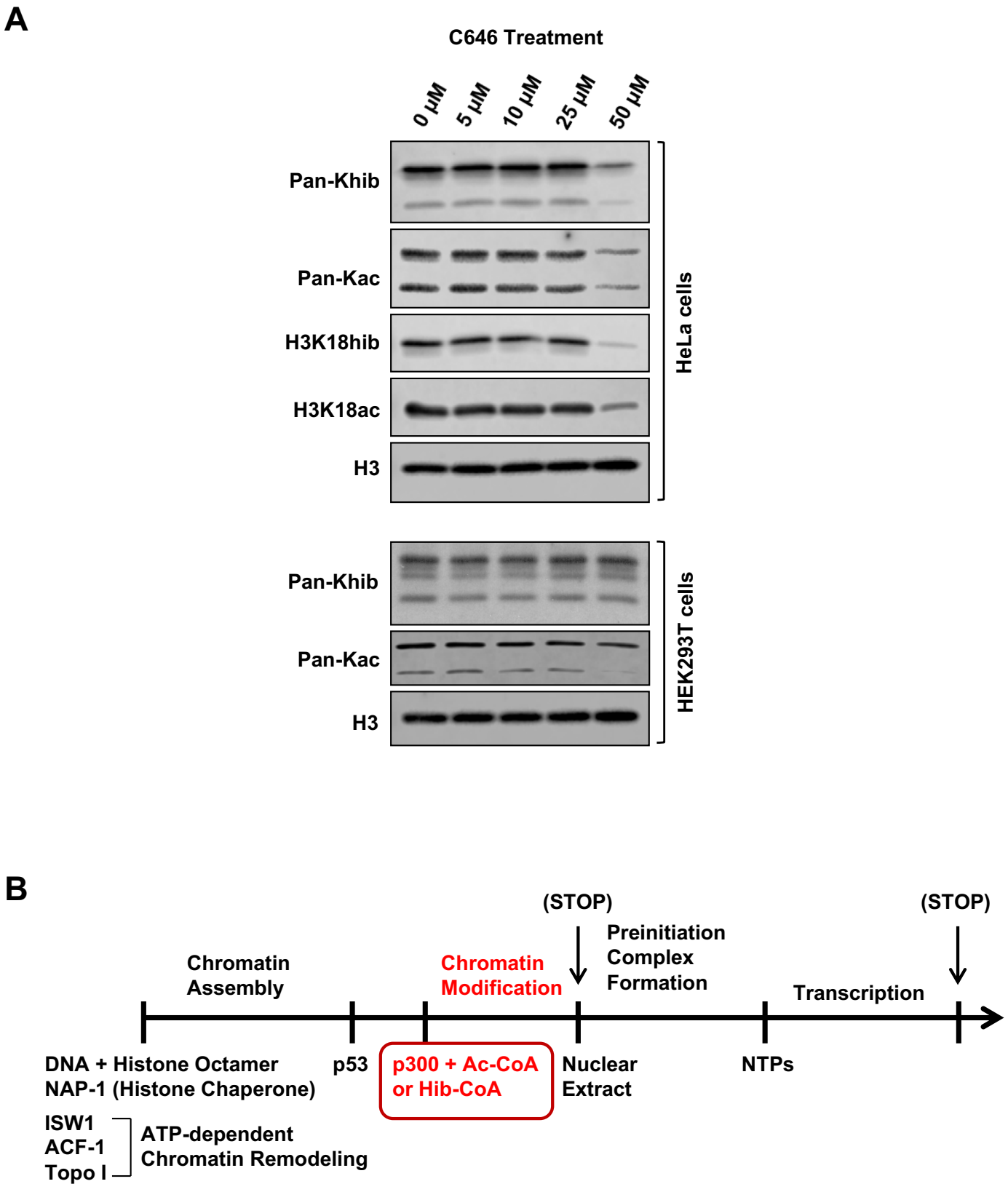
A
C646 Treatment
0 μM
5 μM
10 μM
25 μM
50 μM
Pan-Khib
Pan-Kac
H3K18hib
H3K18ac
H3
HeLa cells
Pan-Khib
Pan-Kac
H3
HEK293T cells
B
(STOP)
(STOP)
Preinitiation Complex Formation
Chromatin Assembly
Chromatin Modification
Transcription
DNA + Histone Octamer
NAP-1 (Histone Chaperone)
p53
p300 + Ac-CoA or Hib-CoA
Nuclear Extract
NTPs
ISW1
ACF-1
Topo I
ATP-dependent Chromatin Remodeling

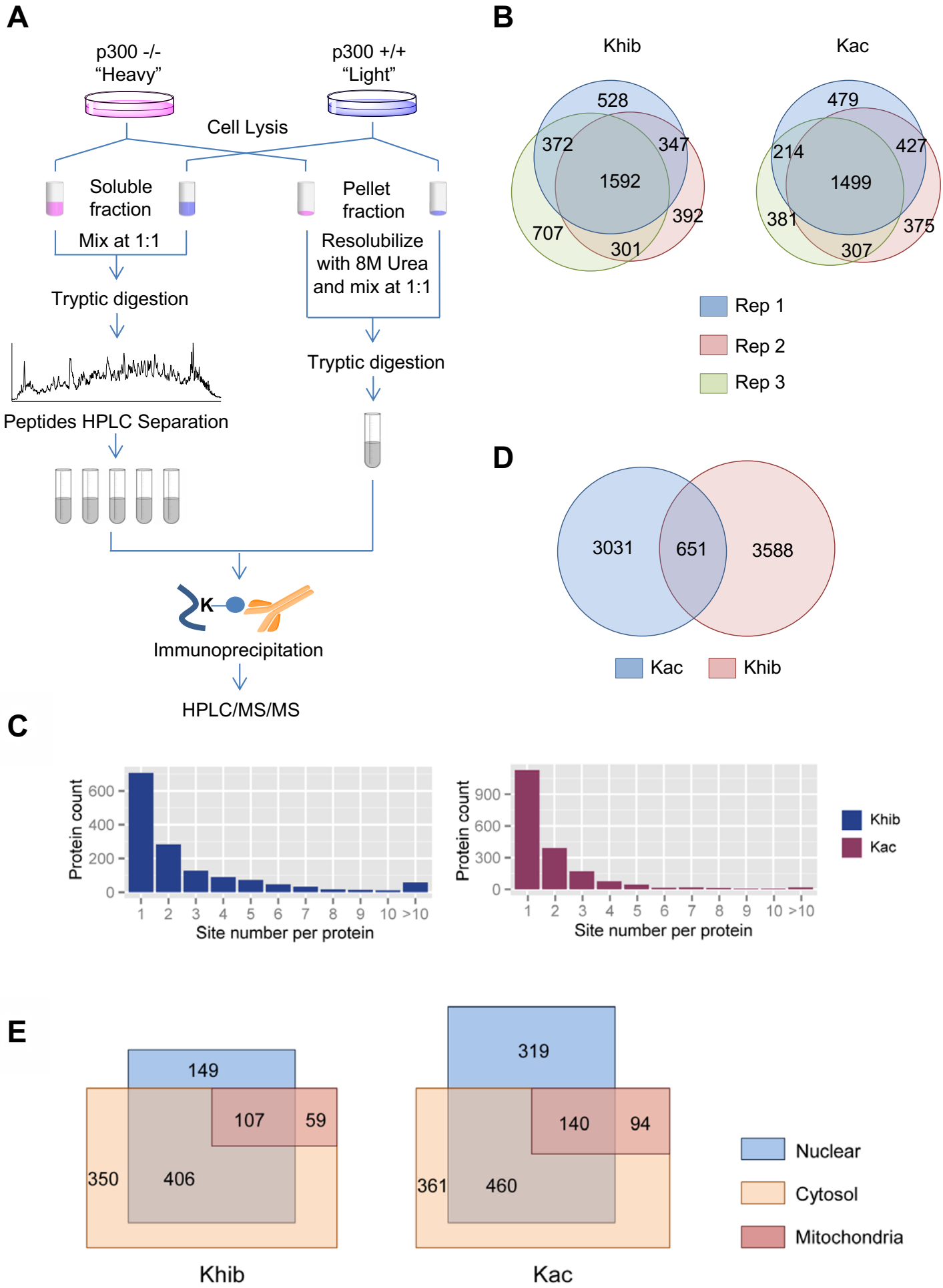
A
p300 -/-
"Heavy"
p300 +/+
"Light"
Cell Lysis
Soluble fraction
Pellet fraction
Mix at 1:1
Resolubilize with 8M Urea and mix at 1:1
Tryptic digestion
Tryptic digestion
Peptides HPLC Separation
K
Immunoprecipitation
HPLC/MS/MS
B
Khib
Kac
528
372
347
1592
392
707
301
479
214
427
1499
381
375
307
Rep 1
Rep 2
Rep 3
D
3031
651
3588
Kac
Khib
C
Protein count
600
400
200
0
1 2 3 4 5 6 7 8 9 10 >10
Site number per protein
Protein count
900
600
300
0
1 2 3 4 5 6 7 8 9 10 >10
Site number per protein
Khib
Kac
E
149
107
59
350
406
Khib
319
140
94
361
460
Kac
Nuclear
Cytosol
Mitochondria

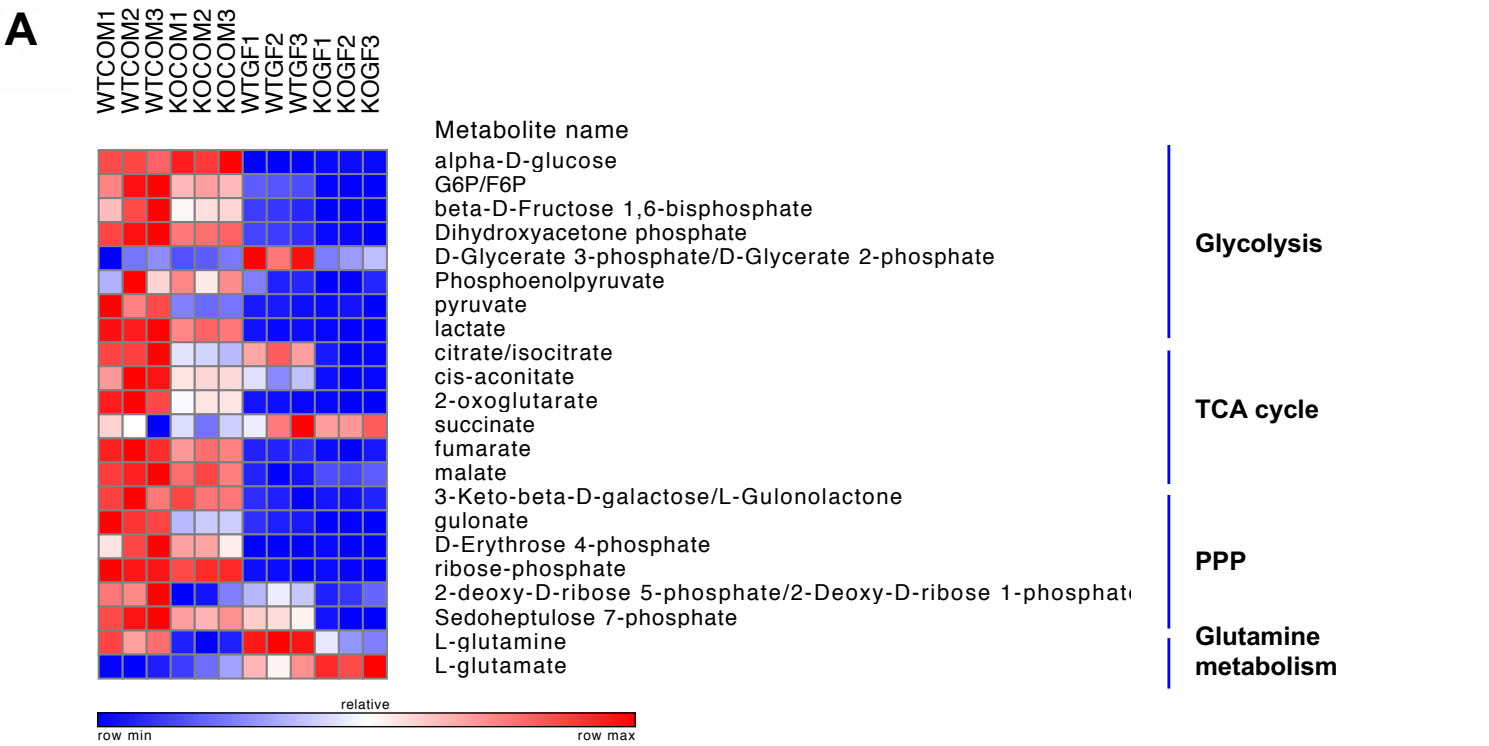
A
WTCOM1
WTCOM2
WTCOM3
KOCOM1
KOCOM2
KOCOM3
WTGF1
WTGF2
WTGF3
KOGF1
KOGF2
KOGF3
Metabolite name
alpha-D-glucose
G6P/F6P
beta-D-Fructose 1,6-bisphosphate
Dihydroxyacetone phosphate
D-Glycerate 3-phosphate/D-Glycerate 2-phosphate
Phosphoenolpyruvate
pyruvate
lactate
citrate/isocitrate
cis-aconitate
2-oxoglutarate
succinate
fumarate
malate
3-Keto-beta-D-galactose/L-Gulonolactone
gulonate
D-Erythrose 4-phosphate
ribose-phosphate
2-deoxy-D-ribose 5-phosphate/2-Deoxy-D-ribose 1-phosphat
Sedoheptulose 7-phosphate
L-glutamine
L-glutamate
Glycolysis
TCA cycle
PPP
Glutamine metabolism
relative
row min
row max

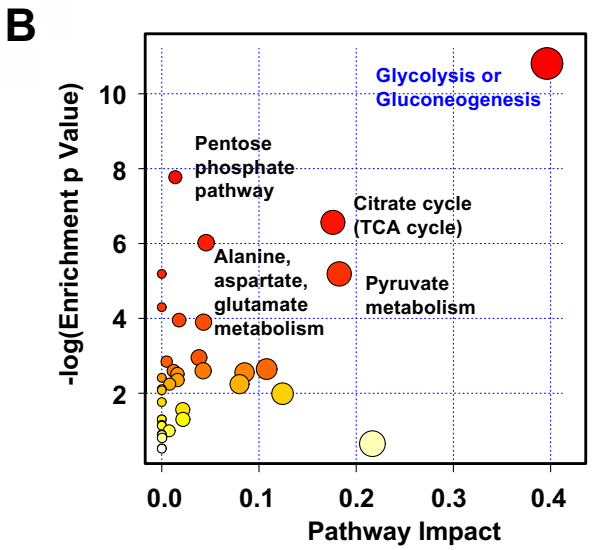
B
-log(Enrichment p Value)
Pathway Impact
Glycolysis or Gluconeogenesis
Pentose phosphate pathway
Citrate cycle (TCA cycle)
Alanine, aspartate, glutamate metabolism
Pyruvate metabolism

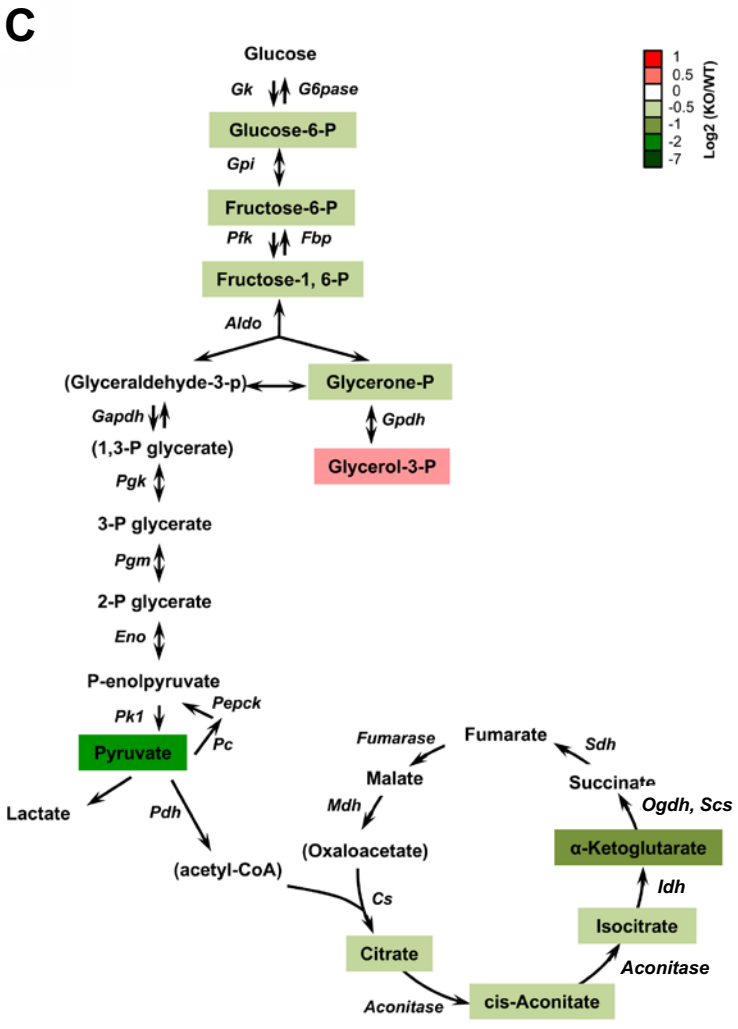
C
Glucose
Gk
G6pase
Glucose-6-P
Gpi
Fructose-6-P
Pfk
Fbp
Fructose-1, 6-P
Aldo
(Glyceraldehyde-3-p)
Glycerone-P
Gapdh
Gpdh
(1,3-P glycerate)
Glycerol-3-P
Pgk
3-P glycerate
Pgm
2-P glycerate
Eno
P-enolpyruvate
Pk1
Pepck
Pc
Pyruvate
Lactate
Pdh
(acetyl-CoA)
Fumarase
Fumarate
Sdh
Malate
Succinate
Mdh
Ogdh, Scs
(Oxaloacetate)
α-Ketoglutarate
Cs
Idh
Citrate
Isocitrate
Aconitase
Aconitase
cis-Aconitate
Log2 (KO/WT)

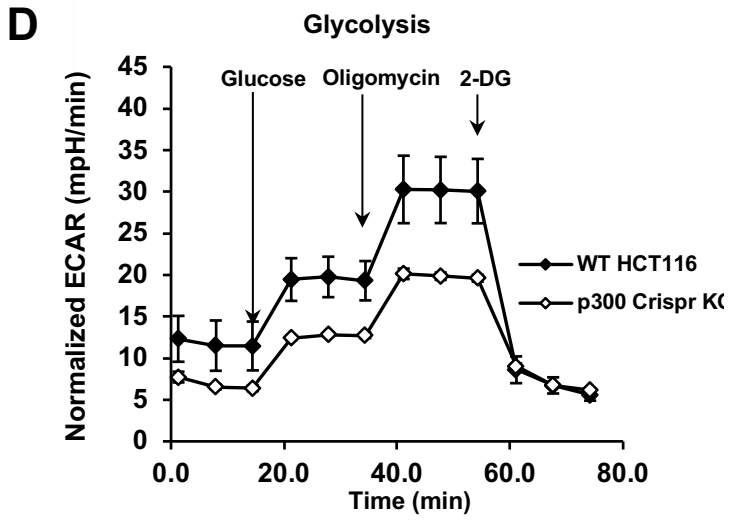
D
Glycolysis
Normalized ECAR (mpH/min)
Time (min)
Glucose
Oligomycin
2-DG
WT HCT116
p300 Crispr KO

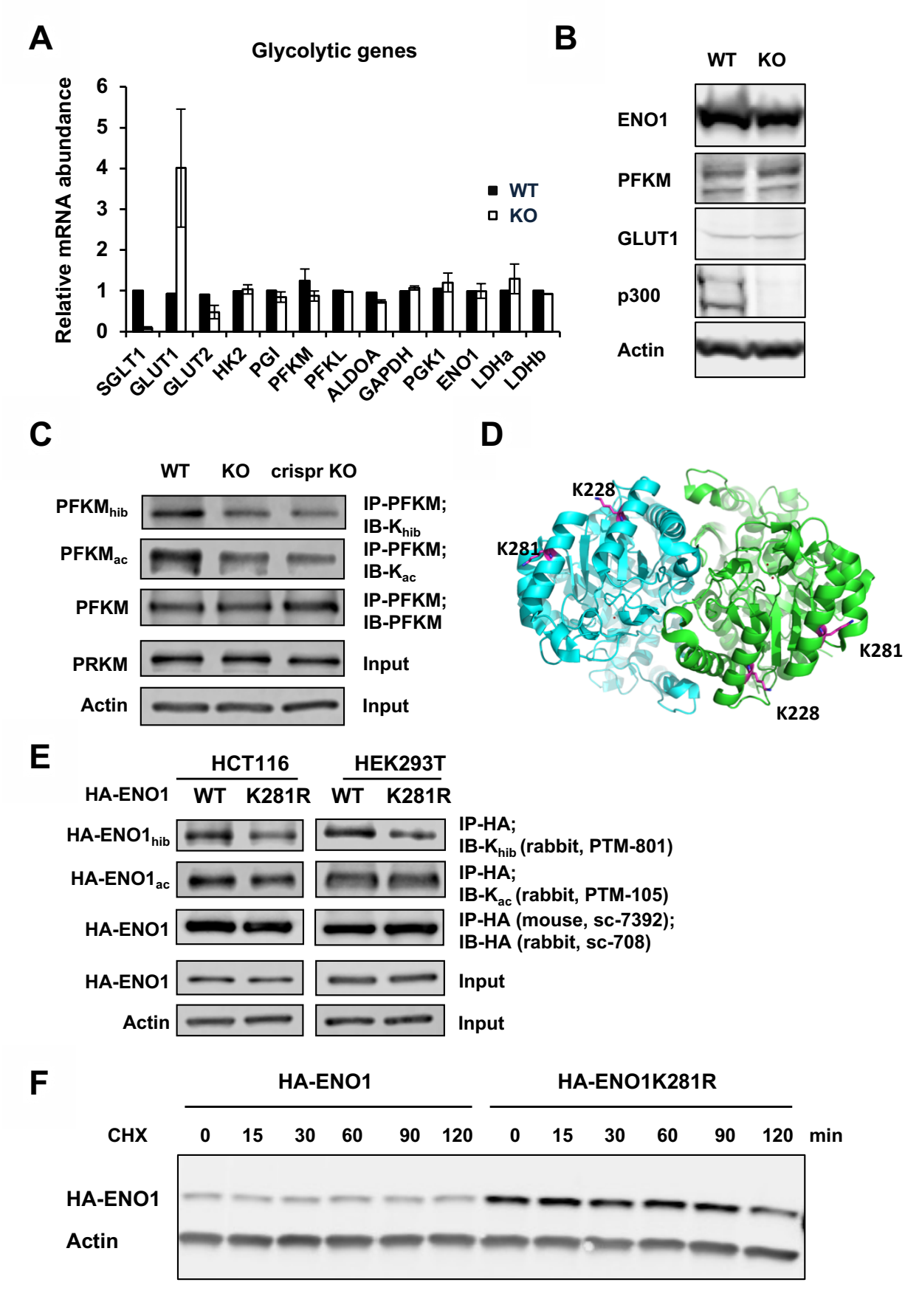
A
Glycolytic genes
Relative mRNA abundance
WT
KO
SGLT1
GLUT1
GLUT2
HK2
PGI
PFKM
PFKL
ALDOA
GAPDH
PGK1
ENO1
LDHa
LDHb
B
WT KO
ENO1
PFKM
GLUT1
p300
Actin
C
WT KO crispr KO
PFKM$_{hib}$
IP-PFKM; IB-K$_{hib}$
PFKM$_{ac}$
IP-PFKM; IB-K$_{ac}$
PFKM
IP-PFKM; IB-PFKM
PRKM
Input
Actin
Input
D
K228
K281
K281
K228
E
HCT116
HEK293T
HA-ENO1
WT K281R WT K281R
HA-ENO1$_{hib}$
IP-HA; IB-K$_{hib}$ (rabbit, PTM-801)
HA-ENO1$_{ac}$
IP-HA; IB-K$_{ac}$ (rabbit, PTM-105)
HA-ENO1
IP-HA (mouse, sc-7392); IB-HA (rabbit, sc-708)
HA-ENO1
Input
Actin
Input
F
HA-ENO1
HA-ENO1K281R
CHX
0 15 30 60 90 120 0 15 30 60 90 120 min
HA-ENO1
Actin

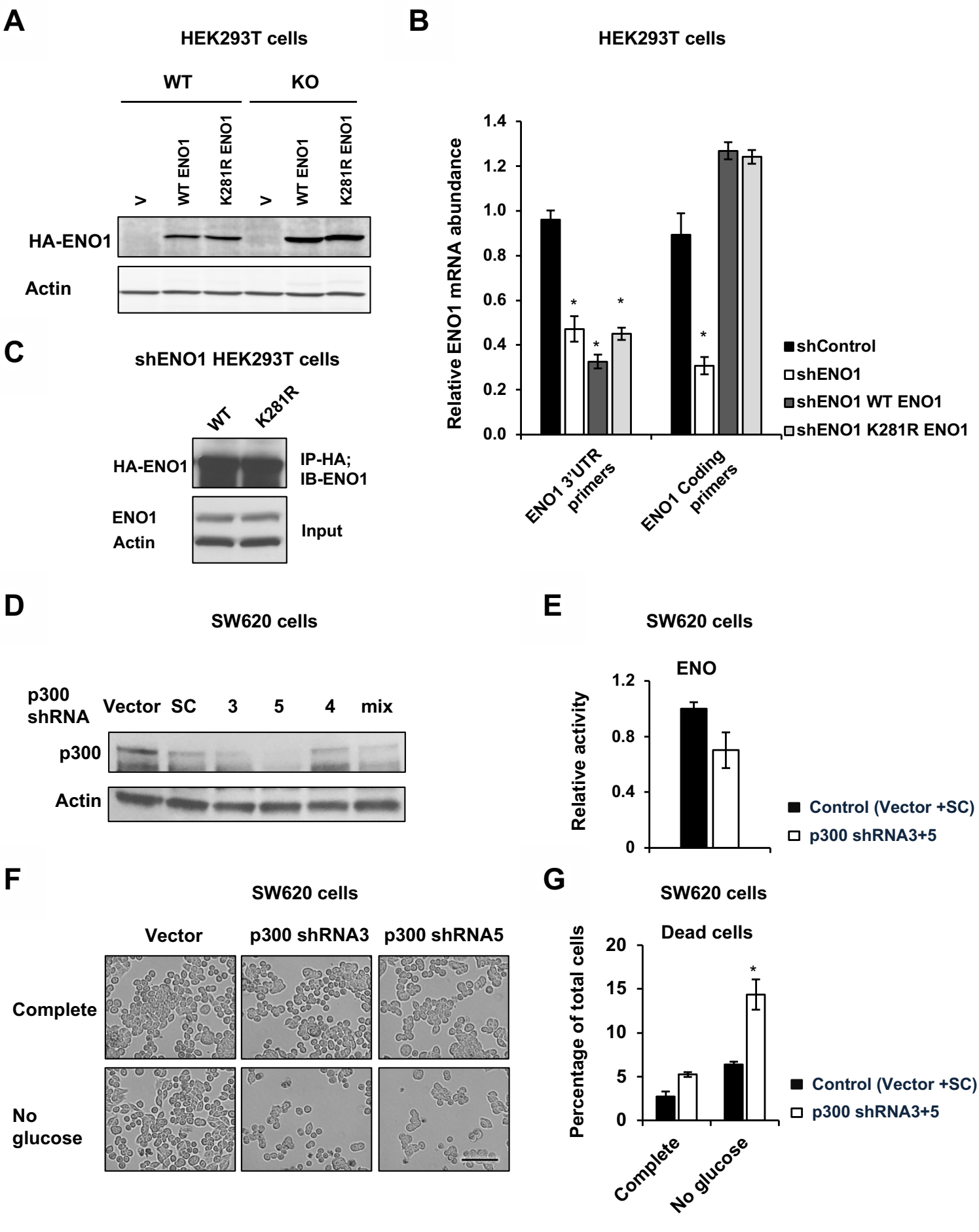
A
HEK293T cells
WT
KO
V
WT ENO1
K281R ENO1
V
WT ENO1
K281R ENO1
HA-ENO1
Actin
B
HEK293T cells
Relative ENO1 mRNA abundance
1.4
1.2
1.0
0.8
0.6
0.4
0.2
0.0
shControl
shENO1
shENO1 WT ENO1
shENO1 K281R ENO1
ENO1 3'UTR primers
ENO1 Coding primers
C
shENO1 HEK293T cells
WT
K281R
HA-ENO1
IP-HA; IB-ENO1
ENO1
Actin
Input
D
SW620 cells
p300 shRNA
Vector
SC
3
5
4
mix
p300
Actin
E
SW620 cells
ENO
Relative activity
1.2
0.8
0.4
0
Control (Vector +SC)
p300 shRNA3+5
F
SW620 cells
Vector
p300 shRNA3
p300 shRNA5
Complete
No glucose
G
SW620 cells
Dead cells
Percentage of total cells
20
15
10
5
0
Control (Vector +SC)
p300 shRNA3+5
Complete
No glucose